



## Deficiency in the Actin Nucleator Cordon Bleu (Cobl) Causes Hypoplastic Enamel in Murine Mandibular Molars

Markus Reise<sup>1</sup>, Markus Heyder<sup>1</sup>, Robert Stemmler<sup>1</sup>, André Güllmar<sup>1</sup>, Natja Haag<sup>2,3</sup>, Michael M. Kessels<sup>2</sup>, Christoph Krafft<sup>4</sup>, Britta Qualmann<sup>2</sup>, Bernd Sigusch<sup>1</sup>, Stefan Kranz<sup>\*,1</sup>

### Abstract

The protein Cordon Bleu (Cobl) belongs to the group of actin nucleators. Through the formation of trimeric actin nuclei, Cobl authorizes the genesis of filamentous actin structures. Cobl has been detected by our group in secretory active and mature ameloblasts. Nevertheless, most aspects of its role in amelogenesis is still unclear. In this study, mandibular molars of 8-13 week old Cobl knock-out (KO) mice (n=6) were collected and enamel samples (n=132) subjected to histomorphometric analysis (quantitative analysis). Enamel composition was investigated by Fourier Transform Infrared spectroscopy (FTIR) and Raman Spectroscopy (qualitative analysis). Results were compared to samples obtained from wild-type mice (WT, n=5). In Cobl KO, reduced absolute (p<0.01) and relative histomorphometric enamel areas (p=0.02) were detected. Cobl KO also showed an increase in enamel-free areas in the molar cusps region. Compared to WT, those defects occurred by an increased probability of 1.323 (p=0.004). FTIR and Raman Spectroscopy revealed no differences in the enamel composition. In summary, Cobl deficiency results in hypoplastic enamel and causes an increase in enamel-free areas. It is assumed that Cobl has a transient influence during the secretory stage of amelogenesis. Further investigations are needed to gain more detailed information on the function of Cobl in these processes.

**Keywords:** Ameloblasts, Amelogenin, Amelogenesis imperfecta, cytoskeleton, Developmental Enamel Defects, Enamel formation, Enamel matrix proteins, F-actin

### Background

Enamel is the hardest and most mineralized human tissue. The process of enamel formation, also known as amelogenesis, is preceded by specialized cells called ameloblasts that first secrete enamel matrix proteins, such as amelogenin, ameloblastin, and enamelin. The secreted protein matrix then interacts with calcium phosphate minerals to form elongated, parallel, and bundled enamel apatite crystals [1,2]. Enamel mineral nucleation and growth is a complex and dynamic set of interactions, which is also associated with functional and morphological cell changes. At the beginning of amelogenesis, presecretory ameloblasts develop into secretory active cells that are highly polarized. One of the most distinct morphological feature of these cells is the occurrence of a triangular shaped cytoplasmic extension located at the distal cell end. This so-called Tomes' process is important for exocytosis mediated vesicle secretion and also determines the boundaries between rod and interrod regions [3].

Once ameloblasts completed the secretory stage, the cells shorten again and assume a more cubic shape with the Tomes processes being also retracted

### Affiliation:

<sup>1</sup>Department of Conservative Dentistry and Periodontology, University Hospitals, Jena, Germany

<sup>2</sup>Institute of Biochemistry I, Jena University Hospital, Friedrich Schiller University, Jena, Germany.

<sup>3</sup>Present address: Institute of Human Genetics, Medical Faculty, RWTH Aachen University, Aachen, Germany.

<sup>4</sup>Leibniz Institute of Photonic Technology (IPHT), Jena, Germany.

### \*Corresponding author:

Stefan Kranz, Department of Conservative Dentistry and Periodontology, University Hospitals, Jena, Germany.

**Citation:** Markus Reise, Markus Heyder, Robert Stemmler, André Güllmar, Natja Haag, Michael M. Kessels, Christoph Krafft, Britta Qualmann, Bernd Sigusch, Stefan Kranz. Deficiency in the actin nucleator Cordon bleu (Cobl) causes hypoplastic enamel in murine mandibular molars. *Fortune Journal of Health Sciences*. 8 (2025): 931-938

**Received:** September 11, 2025

**Accepted:** September 18, 2025

**Published:** October 10, 2025

[4]. These morphological cell changes are mediated by cytoskeleton structures, such as microtubules, intermediate filaments, and actin filaments [5]. Studies have confirmed that especially actin filaments play a major role in such cell transformation processes [6-8]. In enamel matrix secreting ameloblasts, actin filaments are mainly located at the apical cell pole, i.e. in the distal terminal web and also in the Tomes' processes [9-11]. Actin filaments are involved in controlling ameloblast polarity, morphology, and intercellular adhesion which was clearly demonstrated in studies about the role of Rho-associated coiled-coil-containing protein kinase (ROCK) in amelogenesis [12]. Analyses in knock-out (KO) animals have verified that disruption of the RhoA/Rho-associated protein kinase pathway, which is crucial for regulating the actin cytoskeleton, correlates with a reduced expression of amelogenin and also with the formation of hypoplastic enamel defects [13].

Actin filament formation requires the action of actin nucleation factors. Among different types already identified, Cordon-Bleu (Cobl) presents unique properties, especially with regard to amelogenesis [14]. Cobl is an evolutionary relatively young multifunctional WASP-Homology 2 domain-containing nucleator that efficiently promotes the *de novo* synthesis of actin nuclei. It was found that Cobl induces the formation of linear actin structures [15]. Research has shown its importance especially in neuronal morphogenesis, Purkinje cell development and poststroke dendritic arbor regrowth [16-18]. Besides that, Cobl was also identified in epithelial enterocytes of the small intestine, in cochlea hair cells, and recently also in secretory active and mature ameloblasts [14,19-21]. Current research showed the localization of Cobl in the apical cytosol of secretory active ameloblasts. In the same study, it was observed that Cobl deficiency was associated with increased cell height and elevated contents of filamentous actin (F-actin) at the apical membrane of ameloblasts in P0 Cobl KO mice. Compared to WT, mature stage ameloblasts of Cobl KO animals were also afflicted by a significantly reduced intracellular F-actin density. Further, it seems that Cobl also has an influence on the quantity of the formed enamel [14]. In this regard, the present study aimed on completing information about the impact of Cobl on amelogenesis, especially with focus on the quantity and quality of mature enamel in a murine Cobl KO model [20].

## Methods

### Animal model

The study comprised five wild type mice (WT) and six Cobl knock-out (KO) mice specified as Cobl-WH2-KO according to the references [20] and [14]. All animal care and experimental procedures were performed in accordance with the EU animal welfare protection laws and regulations.

The study was approved by a licensing committee from the local government under the permission numbers UKJ-17-021 (Landesamt für Verbraucherschutz, Bad Langensalza, Thuringia, Germany) and twz19-2017 (Stabsstelle Tierschutz, University Hospital, Jena, Thuringia, Germany). Animals were euthanized between 8 and 13 weeks of age. Mandibles were extracted and fixed in 5% paraformaldehyde solution for at least 24 hours. Subsequently, molars with surrounding alveolar bone were collected and air dried for 24 h.

### Sample preparation and documentation

Specimens were embedded in cold-setting embedding resin (EpoFix, Struers GmbH, Willich, Germany). Afterwards, sections of 40–60 µm in thickness were prepared using a bone saw microtome (Leica SP1600, Leica Microsystems GmbH, Wetzlar, Germany) perpendicular to the molars occlusal planes. The sections were fixed on slides using a precision adhesive (Technovit 7200VLC, Heraeus Kulzer GmbH, Hanau, Germany) and subsequently surface polished. In total, 167 sections were obtained from WT and KO. For quantitative analysis, all sections were photographed using a microscope (JENAVAL®, Carl Zeiss MicroImaging GmbH, Jena) in transmitted light mode at 6.3 magnification and a digital camera (AxioCam MRc 5, Carl Zeiss MicroImaging GmbH, Jena, Germany).

### Histomorphometric enamel analysis

In all sections the absolute and relative enamel areas were calculated using ImageJ. The absolute enamel area encompasses the enclosure between the superficial enamel contour and the enamel-dentin junction (Figure 1a). The relative enamel area is defined as ratio of the absolute enamel area to the specimen specific crown area (Figure 1b).

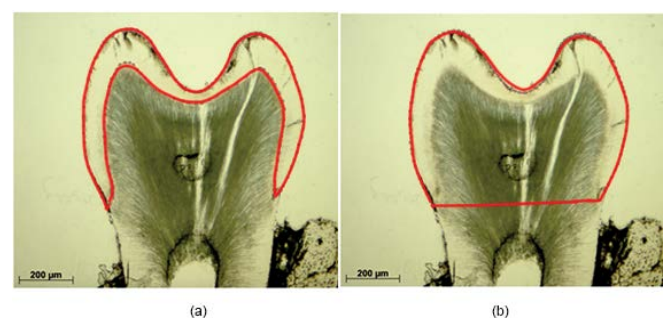


**Figure 1:** (a) Absolute enamel area enclosed by a red line. (b) Specific crown area enclosed by a red line. The ratio of absolute enamel area to specimen specific crown area defines the relative enamel area.

### Enamel-free areas

Enamel-free areas were documented, both, in WT and Cobl KO histological sections. In addition, defects were precisely measured by straight lining of the exposed dentin contour (Figure 2, red line).

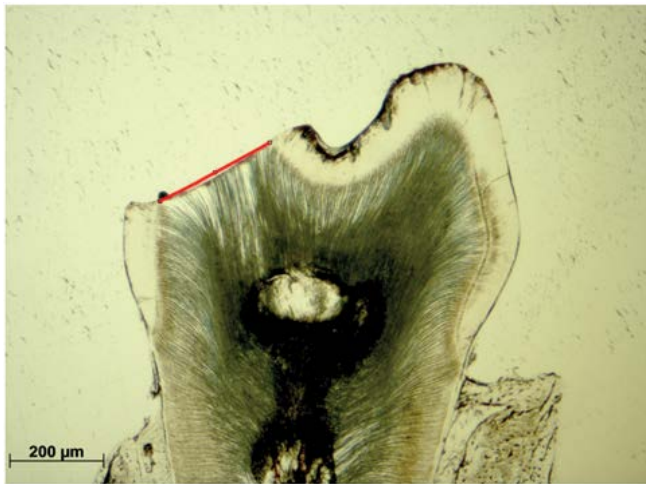


**Figure 2:** Enamel defects measured by lining the exposed dentin contour (straight red line).

### Qualitative enamel analysis by Fourier Transform Infrared (FTIR) spectroscopy

Measurements were performed on transversal cut enamel samples in the cusps region using the Agilent Cary 660 FTIR Spectrometer (Agilent Technologies, Santa Clara, USA) in the range of 900–4000  $\text{cm}^{-1}$  (Figure 3). A germanium attenuated total reflection accessory which was slit on a 15 $\times$  Cassegrain objective lens in the Cary 620 FTIR microscope was pressed onto the enamel until the absorption was maximized. The contact area was 90  $\mu\text{m}$ . As described in an earlier study, a liquid nitrogen cooled single channel mercury cadmium telluride (MCT) detector was used [22]. For analysis Resolution Pro Software, Version 5.4.1 (Agilent Technologies, Santa Clara, USA) was applied. In total, 63 samples were analyzed ( $n = 35$  KO,  $n = 28$  WT).

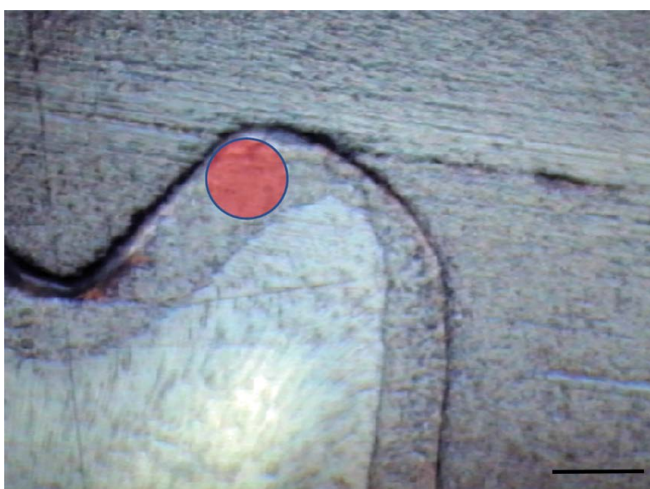


**Figure 3:** FTIR measurement site was marked in red (diameter: 90  $\mu\text{m}$ ). Scale bar 100  $\mu\text{m}$ .

### Qualitative enamel analysis by Raman Spectroscopy

For excitation, a single mode diode laser (Xtra, TOPTICA Photonics AG, Munich, Germany) at 785 nm emission was used which was coupled to a Raman microscope (Microprobe) connected to a Raman spectrometer (RXN1). The instrument was calibrated using a Raman calibration accessory, according to the routines outlined in HoloSpec software, version 4.1.0.234 (all from Kaiser Optical System, Ann Arbor, MI, USA). Measurements were carried out using the objective 100 $\times$ /NA 0.9 (Leica Microsystems, Wetzlar, Germany). For each specimen, 40 individual spectra were recorded with an exposure time of 2 $\times$ 1 seconds along a line at 2  $\mu\text{m}$  intervals (Figure 4). The exposure and measurement times were one second per spectrum each at a wavelength range of 200–3450  $\text{cm}^{-1}$ .

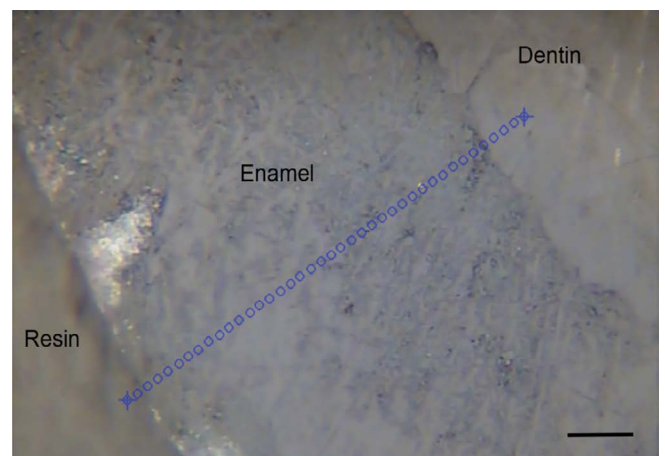


**Figure 4:** Lines of 40 Raman spectra (blue marks, 80  $\mu\text{m}$  in length) were obtained over the spectral region of 200 to 3450  $\text{cm}^{-1}$ . Scale bar 10  $\mu\text{m}$ .

### Statistical analysis

Statistical analysis was performed using SPSS software (IBM, Armonk, New York, USA). A mixed linear regression model was applied with  $p < 0.05$ . The statistical test allowed the assessment of fixed and random effects for a different number of subjects in each group. The aim was to evaluate the influence of the actin nucleator Cobl (fixed effect) on the morphology of enamel in matured murine teeth. The following morphological criteria (random effects) were examined:

- size of enamel area
- probability of an enamel defect
- size of enamel defects

Since the samples each had a maximum of only two enamel defects, this analysis was performed using a generalized estimation equation. Values were presented as means  $\pm$  standard deviation.



## Results

### Histomorphometric enamel analysis

In total, 81 samples were obtained from six Cobl KO and 51 from five WT animals (n=132 in total). Analysis of the enamel quantity showed significant differences between WT and Cobl KO samples. It was found that in Cobl KO the absolute enamel area was significantly reduced. While in WT samples a mean value of  $0.108 \pm 0.029 \text{ mm}^2$  was determined, Cobl KO specimens showed an absolute enamel area of  $0.087 \pm 0.029 \text{ mm}^2$ . This result was significant ( $p < 0.01$ , Figure 5(a)). Cobl KO samples were also afflicted by significantly reduced relative enamel areas. A mean value of  $31.03 \pm 7.61 \%$  was estimated for WT samples, compared to  $26.80 \pm 7.61 \%$  in Cobl KO ( $p = 0.025$ , Figure 5(b)).

In some samples of both groups, enamel-free areas were observed as well. These defects usually occurred isolated in the oral or vestibular cusps region (Figure 6). In all specimens no more than two enamel-free areas occurred simultaneously. It was verified that those defects were more frequently detected in Cobl KO samples as compared to WT. In detail, WT showed a mean defect number of 0.401 relatively to the total number, while in Cobl KO the value increased to 0.769. Both results differed significantly ( $p < 0.001$ ). Furthermore, it was found that enamel-free defects in the cusps regions occurred by an increased probability of 1.323 in Cobl KO animals ( $p = 0.004$ ). In addition, the size of each enamel-free defect was exactly measured. Compared to WT, defects tended to be enlarged in Cobl KO samples. In detail, a mean defect size of  $0.19 \pm 0.11 \text{ mm}$  was determined for WT samples, while in Cobl KO specimens the value increased to  $0.22 \pm 0.15 \text{ mm}$ . However, direct comparison of both groups did not reveal any significant difference among both defect sizes ( $p = 0.51$ , Figure 5(c)).

### Qualitative Enamel Analysis

In Figure 7 results of the Fourier transform infrared spectroscopy (FTIR spectroscopy,  $750\text{--}1750 \text{ cm}^{-1}$ ) and Raman spectroscopy ( $600\text{--}1800 \text{ cm}^{-1}$ ) are presented. Both analysis of mean spectra did not show any differences in enamel crystallinity and mineral composition between WT and Cobl KO samples. In detail, FTIR spectra in the range of  $800\text{--}1200 \text{ cm}^{-1}$  refer to inorganic components. Weak signals were also detected from organic components in the range of  $1200\text{--}1700 \text{ cm}^{-1}$ . Signals between  $860\text{--}880 \text{ cm}^{-1}$  originate from carbonate substitutions, with maxima at  $877 \text{ cm}^{-1}$ , while peaks in the range of  $1415$  and  $1456 \text{ cm}^{-1}$  are from type B carbonates. Hydrogen phosphate is represented by signals at  $1009 \text{ cm}^{-1}$ , whereas peaks at  $960 \text{ cm}^{-1}$  can be referred to phosphates in the hydroxyl apatite. There were no significant differences in the FTIR signals between WT and Cobl KO.

In Raman spectroscopy, relative intensity at  $960 \text{ cm}^{-1}$  represents the stretching vibration  $\nu_1$  of the phosphate band.

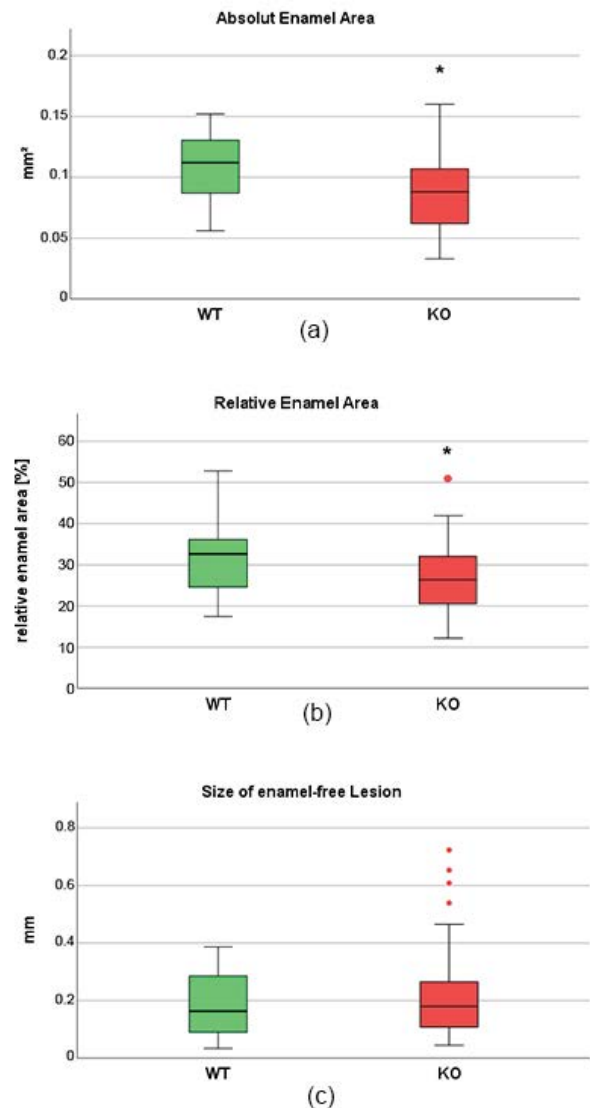


**Figure 5:** Results of the quantitative histomorphometric analysis of wild type (WT, n=51) and Cobl knock-out (KO, n=81) murine enamel samples. (a) Absolute enamel area, (b) relative enamel area, (c) size of enamel-free defects. Mixed linear regression model showed significance between WT and Cobl KO for the absolute ( $p < 0.01$ ) and relative enamel area ( $p = 0.025$ ), which is indicated by stars. Red dots represent outliers.

The width of this band is a marker for crystallinity which did not show significant changes. Peaks at  $1074 \text{ cm}^{-1}$  correspond to the  $\nu_1$  vibration of carbonate, while peaks at  $817$ ,  $1074$ , and  $1454 \text{ cm}^{-1}$  originate from collagens. Although no collagen contributions are expected in enamel, weak signals of organic materials are consistent in mean spectra including dentin and resin at the margin of the lines as evident in Figure 4 [23]. Signals such as those from hydrogen phosphate were detected only to a weak extent. Same as the FTIR-analysis, no significant differences between WT and Cobl KO were found in Raman spectroscopy. All results obtained from FTIR and Raman spectroscopy are also summarized in Table 1.



**Figure 6:** Cobl KO sample with two enamel-free defects in the vestibular and oral cusps region.

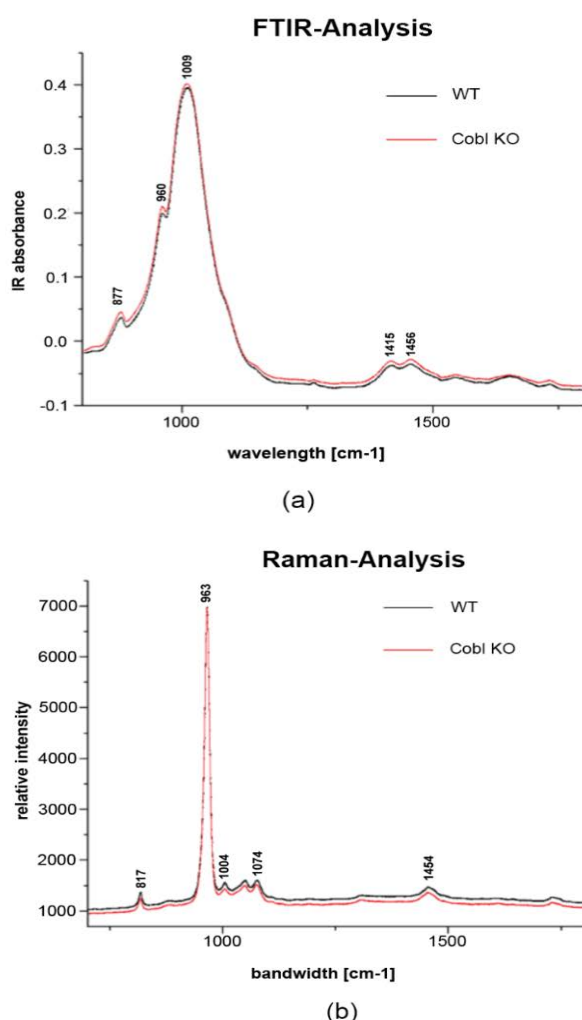


**Figure 7:** FTIR (a) and Raman spectra (b) of Cobl KO and WT tooth samples. Red lines represent signals obtained from Cobl knock-out (KO) samples, while WT is shown in black. In both analysis no significant differences between WT and Cobl KO were detected.

## Analysis of enamel carbonates

FTIR spectra at 860  $\text{cm}^{-1}$  correlates with the  $\nu_2$  vibration of type A2 carbonate. Additional peaks were also recorded at 870 and 878  $\text{cm}^{-1}$ , which are attributable to the  $\nu_2$  vibration of A- and B-type carbonate. Carbonate substitution on the phosphates of apatite (type B carbonate) predominates in both groups (table 2). Nevertheless, no significant differences in the substitution ratio was observed between Cobl KO and WT. In conclusion, knockout of the actin nucleator Cobl has no significant impact on enamel carbonate substitution in mice.

**Table 1:** Summary of signals obtained from FTIR and Raman spectroscopy of enamel.

FTIR spectroscopy		Raman spectroscopy	
[ $\text{cm}^{-1}$ ]	assignment	[ $\text{cm}^{-1}$ ]	assignment
877	$\nu_2 \text{CO}_3^{2-}$	817	collagen
960	$\nu_1 \text{PO}_4^{3-}$	963	$\nu_1 \text{PO}_4^{3-}$
1009	$\text{HPO}_4^{2-}$	1004	collagen
1415; 1454	Type B $\text{CO}_3^{2-}$	1074	$\nu_1 \text{CO}_3^{2-}$
		1454	collagen

**Table 2:** Substituted carbonates in enamel apatite

Wavelength [nm]	Type of carbonate	Carbonate content in apatite [%]	
		WT	Cobl KO
860	A2	18.3	22.4
870	B	67.6	62.6
878	A	14.1	15

## Discussion

The protein Cordon Bleu (Cobl), along with the Arp2/3 complex and formins, belongs to the group of actin nucleators. Through the formation of trimeric actin nuclei, Cobl authorizes the genesis of filamentous actin (F-actin) structures [24]. Immunohistochemical studies have shown that Cobl is also present in ameloblasts of tooth germs in mice [14]. The results of the present murine model demonstrated that knock-out (KO) of Cobl has a significant impact on enamel morphology. As shown by the results, Cobl-deficiency was associated with a significant reduction in enamel quantity. Compared to wildtype (WT) samples, histomorphometric analysis revealed significant reduced values for the absolute and relative enamel areas. Additionally, hypoplastic enamel defects in the oral and vestibular cusps region were found to occur to a significant higher extent. The results of the present investigation differ from our data published recently about the function of Cobl in amelogenesis. In contrary to the results of the present study, a significant increase in enamel quantity among P10 (postnatal day 10) Cobl KO murine molar samples was reported [14]. Detailed examinations

verified that the histomorphometric ratio of enamel area to tooth crown area was significantly increased compared to WT [14]. The differences in enamel quantity between both studies might be due to the fact that in the present investigation mature molars from animals aged 8-13 weeks were investigated and not teeth of the developmental stage P10. At P10, murine molars just start to erupt and maturation is not yet completed [25]. Investigations have also verified that there are high morphological differences between individual molars in mice which might be another possible reason for the mismatch in the observed parameters [26,27].

In the present investigation Cobl KO samples also showed isolated hypoplastic enamel defects located in the oral and vestibular cusps region. In all specimens no more than two enamel defects were detected simultaneously. Up to now, there is no study available that confirms an association between Cobl deficiency and the occurrence of hypo- or aplastic enamel lesions. At the current state, it is assumed that the observed defects have already existed at the time of eruption and enlarged due to attrition. As already known, enamel thickness and structure in mouse molars show regional variations. Besides that, so called enamel-free areas in the cusps region of murine molars are commonly found at the time of eruption [26]. Anyhow, results from the present study confirm that enamel-free lesions were detected to a much higher frequency in Cobl KO as compared to WT animals of the same age. Compared to WT those defects occurred by a probability of 1.323 in Cobl KO mice. Hypoplastic enamel defects prior to tooth eruption are almost exclusively associated with insufficiencies during the secretory stage of amelogenesis. Any pathological alterations during enamel formation (hereditary, systemic, acquired, local etiological factors), might cause the manifestation of flaws in the structure, known as Developmental Enamel Defects [28].

In this regard, recent data about the influence of Cobl on amelogenesis clearly demonstrates that the cell morphology of ameloblasts is significantly affected by Cobl deficiency. In detail, it was reported that in the secretory stage (P0) of Cobl KO samples, ameloblasts were characterized by a significant increase in height. The changes were found to be most pronounced in the cusp-equator area and in the fissure-cusp region. Furthermore, the same study observed a significantly increased mean F-actin intensity in P0 Cobl KO samples along the apical membrane region of ameloblasts in the cusp area, whereas at P10 the actin cytoskeleton in the apical membrane zone was severely impaired and showed a dramatic lack of F-actin [14]. It can be assumed that changes in the cell morphology and particularly in the F-actin content upon Cobl KO can be considered causative factors for the occurrence of hypoplastic and aplastic enamel lesions. If such changes are also linked to an altered secretion of enamel matrix proteins, still needs to be examined in detail. Important

insights into this topic have been provided already by a study published in 2013 about RhoA deficiency in transgenic mice. The results proved that in animals with impaired actin formation, amelogenin production was significantly reduced. Furthermore, all animals with RhoA-deficiency showed hypoplastic enamel defects as well [13]. Recent data also verified the importance of other regulator molecules such as mTOR or Smurf1, which have a distinct influence on actin mediated cytoskeletal functions and, thus, enamel formation [29,30].

Besides changes in the enamel quantity, no differences in the organic (very small quantity) or mineral composition between Cobl KO and WT were detected in the present investigation, neither by FTIR analysis nor by Raman spectroscopy. As outlined above, the process of enamel maturation, which follows the secretory stage, is crucial for determining final enamel mineral quality. During this phase, calcium, phosphate, and bicarbonates are deposited in exchange with water and organic molecules [31]. The results of the present study indicate that the processes of enamel maturation is not effected by Cobl deficiency. This supports the assumption that Cobl might only have a transient effect on amelogenesis, limited to the secretory stage. Similar results were also obtained from studies on amelogenin-deficient mice. Although these mice were characterized by hypoplastic, disorganized enamel, their mineral composition remained unaffected [32]. In contrast to the observed results of the present study, however, current data of our group indicate significant deviations in the enamel carbon content between WT and Cobl KO [14]. In detail, it was found that under Cobl deficiency the carbon concentration in P10 enamel molar samples was significantly increased by 20% compared to WT. The phenotype of increased carbon content in the enamel of Cobl-KO mice was also evident when the enamel layers were analyzed separately, as inner and outer enamel regions had similar elemental compositions [14].

## Conclusion

The findings of the present investigation have demonstrated that the actin nucleator Cobl seems to have distinct influence on enamel formation in the secretory stage of amelogenesis, while organic and inorganic enamel composition is not affected. Further studies are needed to confirm the discussed and assumed functions of Cobl in amelogenesis. To make statements about possible targeted structures, it seems worthwhile to investigate the spatial and temporal expression pattern of Cobl. One approach might be to perform conditional knock-out experiments, in which Cobl is temporarily and spatially deactivated. Direct detection of F-actin, the effector structure of Cobl, also allows for a spatial and temporal classification of the actin nucleator during amelogenesis. Experiments should also proof if Cobl has a

significant impact on the secretion of enamel matrix proteins during the secretory stage of amelogenesis.

## Acknowledgement

We gratefully acknowledge all employees of the Biochemistry Institute I, University Hospital, Jena, Germany that were involved in this study. This work was supported by grants from the German Research Foundation (KE685/3).

## Ethical Consideration

This research was approved by a licensing committee from the local government under the permission numbers UKJ-17-021 (Landesamt für Verbraucherschutz, Bad Langensalza, Thuringia, Germany) and twz19-2017 (Stabsstelle Tierschutz, University Hospital, Jena, Thuringia, Germany).

## Declaration of Competing Interest

All authors declare no potential conflicts of interest with respect to the research, authorship, and/or publication of this article.

## CRedit Authorship Contribution Statement

**Markus Reise:** Writing – Review and Editing

**Markus Heyder:** Writing – Review and Editing

**Robert Stemmler:** Writing – Review and Editing, Formal analysis, Investigation, Data curation, Formal analysis

**André Güllmar:** Writing – Review and Editing, Formal analysis, Investigation, Data curation, Visualization

**Natja Haag:** Methodology, Review and Editing, Formal analysis, Investigation, Data curation, Visualization

**Michael M. Kessels:** Supervision, Investigation, Methodology, Data curation, Funding

**Christoph Krafft:** Supervision, Investigation, Data curation, Visualization, Writing – Review and Editing

**Britta Qualmann:** Supervision, Methodology, Review and Editing

**Bernd Sigusch:** Supervision, Review and Editing

**Stefan Kranz:** Writing – Review and Editing, Formal analysis, Investigation, Data curation, Writing-Original draft preparation, Visualization

## Data Availability

Data can be obtained on request from the corresponding author.

## References

1. Pandya M, Diekwisch TGH. Amelogenesis: Transformation of a protein-mineral matrix into tooth enamel. *J Struct Biol* 213 (2021): 107809.
2. Bartlett JD. Dental Enamel Development: Proteinases and Their Enamel Matrix Substrates. *International Scholarly Research Notices* 2013 (2013): 684607.
3. Lacruz RS, Habelitz S, Wright JT, Paine ML. DENTAL ENAMEL FORMATION AND IMPLICATIONS FOR ORAL HEALTH AND DISEASE. *Physiol Rev* 97 (2017): 939-993.
4. Bartlett JD. Dental enamel development: proteinases and their enamel matrix substrates. *ISRN Dent* 2013 (2013): 684607.
5. Nishikawa S. Cytoskeleton, intercellular junctions, planar cell polarity, and cell movement in amelogenesis. *Journal of Oral Biosciences* 59 (2017): 197-204.
6. Mohapatra S, Wegmann S. Biomolecular condensation involving the cytoskeleton. *Brain Res Bull* 194 (2023): 105-117.
7. Pollard TD, Cooper JA. Actin, a central player in cell shape and movement. *Science* 326 (2009): 1208-1212.
8. Svitkina T. The Actin Cytoskeleton and Actin-Based Motility. *Cold Spring Harb Perspect Biol* 10 (2018).
9. Nishikawa S, Kitamura H. Localization of actin during differentiation of the ameloblast, its related epithelial cells and odontoblasts in the rat incisor using NBD-phalloidin. *Differentiation* 30 (1986): 237-243.
10. Lesot H, Meyer JM, Ruch JV, Weber K, Osborn M. Immunofluorescent localization of vimentin, prekeratin and actin during odontoblast and ameloblast differentiation. *Differentiation* 21 (1982): 133-137.
11. Diekwisch T. Localization of microfilaments and microtubules during dental development in the rat. *Acta Histochem Suppl* 37 (1989): 209-212.
12. Otsu K, Kishigami R, Fujiwara N, Ishizeki K, Harada H. Functional role of Rho-kinase in ameloblast differentiation. *J Cell Physiol* 226 (2011): 2527-2534.
13. Xue H, Li Y, Everett ET, Ryan K, Peng L, Porecha R, Yan Y, Lucchese AM, Kuehl MA, Pugach MK, Bouchard J, Gibson CW. Ameloblasts require active RhoA to generate normal dental enamel. *Eur J Oral Sci* 121 (2013): 293-302.
14. Janitzek H, González Delgado J, Haag N, Seemann E, Nietzsche S, Sigusch B, Qualmann B, Kessels MM. The Evolutionary Young Actin Nucleator Cobl Is Important for Proper Amelogenesis. *Cells* 14 (2025).
15. Grega-Larson NE, Crawley SW, Tyska MJ. Impact of cordon-bleu expression on actin cytoskeleton architecture and dynamics. *Cytoskeleton (Hoboken)* 73 (2016): 670-679.



16. Haag N, Schwintzer L, Ahuja R, Koch N, Grimm J, Heuer H, Qualmann B, Kessels MM. The actin nucleator Cobl is crucial for Purkinje cell development and works in close conjunction with the F-actin binding protein Abp1. *J Neurosci* 32 (2012): 17842-17856.
17. Ji Y, Koch D, González Delgado J, Günther M, Witte OW, Kessels MM, Frahm C, Qualmann B. Poststroke dendritic arbor regrowth requires the actin nucleator Cobl. *PLoS Biol* 19 (2021): e3001399.
18. Kessels MM, Schwintzer L, Schlobinski D, Qualmann B. Controlling actin cytoskeletal organization and dynamics during neuronal morphogenesis. *Eur J Cell Biol* 90 (2011): 926-933.
19. Beer AJ, González Delgado J, Steiniger F, Qualmann B, Kessels MM. The actin nucleator Cobl organises the terminal web of enterocytes. *Sci Rep* 10 (2020): 11156.
20. Haag N, Schüler S, Nietzsche S, Hübner CA, Strenzke N, Qualmann B, Kessels MM. The Actin Nucleator Cobl Is Critical for Centriolar Positioning, Postnatal Planar Cell Polarity Refinement, and Function of the Cochlea. *Cell Rep* 24 (2018): 2418-2431.e2416.
21. Lacruz RS, Smith CE, Bringas P, Jr., Chen YB, Smith SM, Snead ML, Kurtz I, Hacia JG, Hubbard MJ, Paine ML. Identification of novel candidate genes involved in mineralization of dental enamel by genome-wide transcript profiling. *J Cell Physiol* 227 (2012): 2264-2275.
22. Anwar Alebrahim M, Krafft C, Sekhaneh W, Sigusch B, Popp J. ATR-FTIR and Raman spectroscopy of primary and permanent teeth. *Biomedical Spectroscopy and Imaging* 3 (2014): 15-27.
23. Kranz S, Heyder M, Mueller S, Guellmar A, Krafft C, Nietzsche S, Tschirpke C, Herold V, Sigusch B, Reise M. Remineralization of Artificially Demineralized Human Enamel and Dentin Samples by Zinc-Carbonate Hydroxyapatite Nanocrystals. *Materials (Basel)* 15 (2022).
24. Ahuja R, Pinyol R, Reichenbach N, Custer L, Klingensmith J, Kessels MM, Qualmann B. Cordon-bleu is an actin nucleation factor and controls neuronal morphology. *Cell* 131 (2007): 337-350.
25. Lungová V, Radlanski RJ, Tucker AS, Renz H, Mišek I, Matalová E. Tooth-bone morphogenesis during postnatal stages of mouse first molar development. *J Anat* 218 (2011): 699-716.
26. Lyngstadaas SP, Møinichen CB, Risnes S. Crown morphology, enamel distribution, and enamel structure in mouse molars. *Anat Rec* 250 (1998): 268-280.
27. Jiang Y, Katsura KA, Badt NZ, et al. Multi-modal characterization of rodent tooth development (2024).
28. Paschoal MaB, Andrade-Maia G, Cristine-Silva L, Nogueira AF, Miranda F, Garib D. Developmental enamel defects: a must-know for orthodontic practice. *Dental Press J Orthod* 30 (2025): e25spe22.
29. Nie X, Zheng J, Cruciger M, Yang P, Mao JJ. mTOR plays a pivotal role in multiple processes of enamel organ development principally through the mTORC1 pathway and in part via regulating cytoskeleton dynamics. *Dev Biol* 467 (2020): 77-87.
30. Niu H, Bi F, Zhao W, Xu Y, Han Q, Guo W, Chen Y. Smurf1 regulates ameloblast polarization by ubiquitination-mediated degradation of RhoA. *Cell Prolif* 56 (2023): e13387.
31. Simmer JP, Papagerakis P, Smith CE, Fisher DC, Rountrey AN, Zheng L, Hu JC. Regulation of dental enamel shape and hardness. *J Dent Res* 89 (2010): 1024-1038.
32. Gibson CW, Yuan ZA, Hall B, Longenecker G, Chen E, Thyagarajan T, Sreenath T, Wright JT, Decker S, Piddington R, Harrison G, Kulkarni AB. Amelogenin-deficient mice display an amelogenesis imperfecta phenotype. *J Biol Chem* 276 (2001): 31871-31875.



This article is an open access article distributed under the terms and conditions of the [Creative Commons Attribution \(CC-BY\) license 4.0](https://creativecommons.org/licenses/by/4.0/)